

The 250 °C range in temperature inferred from measurements of BTT is similar in magnitude to the range calculated from variations in the independent P-wave velocity model. The general trend in the locations of the peak thermal anomalies derived from both methods correlate well.

Computation of seismic velocity profiles from mineral physics data suggests that multiple transitions are present, and are most distinct at low temperatures such as those associated with subduction zones<sup>4</sup>. The additional boundaries are due to the garnet transformations to ilmenite (shallower than 660 km) and perovskite (deeper than 660 km). At subduction temperatures, mineral physics calculations suggest that distinct transitions occur at 608–664, 690–693 and 709–731 km. The existence of these three discontinuities has also been suggested by a seismic investigation of the subduction zone beneath northeast China where three distinct discontinuities between 660 and 780 km are found at the tip of the subducting slab<sup>21</sup>. Our interpreted depth variation from 730 to 750 km of the proposed garnet phase change requires almost one-third of the temperature anomaly suggested for the slab beneath China. Other seismic investigations found seismic signatures near the 660-km depth that were inconsistent with a simple transformation in a simple olivine system<sup>13,22,23</sup>, which suggests that the base of the transition zone is not simply a dissociation of  $\gamma$ -spinel.

Southern California has been exposed to a spectrum of tectonic events which has created a thermally complex region to study (characterized by the recent subduction of a relatively cold oceanic slab followed by the subduction of a warm spreading ridge with possible continued down welling of cold upper mantle material along the transverse ranges). Observed variations in the BTT between the 660 and 720 km discontinuities (associated with the dissociation of olivine and garnet phases, respectively) beneath this thermally complex region supports the hypothesis that significant garnet transformations exist near the base of the upper mantle transition zone. The anticorrelated depth variations of these discontinuities are in agreement with the garnet–olivine systems proposed near a depth of 660 km. Calculations of the thermal anomalies based on the observed BTT are similar to those derived from an independent tomography model. These observations suggest that garnet phases must be considered when studying the base of the transition zone in thermally complex regions such as southern California and in regions with subducted slabs<sup>21</sup>. To determine the relative significance of garnet phase transformations coupled with olivine transformations, as global processes, will require additional work in less complex regions. □

Received 12 November 1999; accepted 10 April 2000.

1. Ringwood, A. E. in *Advances in Earth Sciences* (ed. Hurley, P. M.) 287–356 (MIT Press, Cambridge, Massachusetts, 1966).
2. Ito, E. & Takahasi, E. Postspinel transformations in the system Mg<sub>2</sub>SiO<sub>4</sub>–Fe<sub>2</sub>SiO<sub>4</sub>, and some geophysical implications. *J. Geophys. Res.* **94**, 10637–10646 (1989).
3. Ito, E., Akaogi, M., Topor, L. & Navrotsky, A. Negative pressure–temperature slopes for reactions forming MgSiO<sub>3</sub> perovskite from calorimetry. *Science* **249**, 1275–1278 (1990).
4. Vacher, P., Mocquet, A. & Sotin, C. Computation of seismic profiles from mineral physics: the importance of the non-olivine components for explaining the 660 km depth discontinuity. *Phys. Earth Planet. Inter.* **106**, 275–298 (1998).
5. Herzberg, C. & Gasparik, T. Garnet and pyroxenes in the mantle: a test of the majorite fractionation hypothesis. *J. Geophys. Res.* **96**, 16263–16274 (1991).
6. Gasparik, T. Enstatite-jadeite join and its role in the Earth's mantle. *Contrib. Mineral. Petrol.* **111**, 283–298 (1992).
7. Gasparik, T. Melting experiments on the enstatite–diopside join at 70–224 kbar, including the melting of diopside. *Contrib. Mineral. Petrol.* **124**, 139–153 (1996).
8. Gasparik, T. A model for the layered upper mantle. *Phys. Earth Planet. Inter.* **100**, 197–212 (1997).
9. Weidner, D. J. & Wang, Y. Chemical- and Clapeyron-induced buoyancy at the 660 km discontinuity. *J. Geophys. Res.* **103**, 7431–7441 (1998).
10. Ringwood, A. E. Role of the transition zone and 660 km discontinuity in mantle dynamics. *Phys. Earth Planet. Inter.* **86**, 5–24 (1994).
11. Dueker, K. G. & Sheehan, A. F. Mantle discontinuity structure beneath the Colorado Rocky Mountains and High Plains. *J. Geophys. Res.* **103**, 7153–7169 (1998).
12. Li, A., Fisher, K. M., Wyssession, M. E. & Clarke, T. J. Mantle discontinuity and temperature under the North American continental keel. *Nature* **395**, 160–163 (1998).
13. Owens, T. J., Nyblade, A. A., Gurrrola, H. & Langston, C. A. 410 and 660 km discontinuity structure beneath Tanzania, East Africa. *Geophys. Res. Lett.* **27**, 827–830 (2000).

14. Owens, T. J., Zandt, G. & Taylor, S. R. Seismic evidence for an ancient rift beneath the Cumberland Plateau, Tennessee: a detailed analysis of broadband teleseismic P-waveforms. *J. Geophys. Res.* **89**, 7783–7795 (1984).
15. Ammon, C. J. The isolation of receiver effects from teleseismic P waveforms. *Bull. Seismol. Soc. Am.* **81**, 2504–2510 (1991).
16. Kennett, B. L. N. & Engdahl, E. R. Traveltimes for global earthquake location and phase identification. *Geophys. J. Int.* **105**, 429–465 (1991).
17. Van der Lee, S. & Nolet, G. Upper mantle S-velocity structure of North America. *J. Geophys. Res.* **102**, 22815–22838 (1997).
18. Stixtrude, L. Structure and sharpness of phase transitions and mantle discontinuities. *J. Geophys. Res.* **102**, 14835–14852 (1997).
19. Weidner, D. J. & Wang, Y. Chemical- and Clapeyron-induced buoyancy at the 660 km discontinuity. *J. Geophys. Res.* **103**, 7431–7441 (1998).
20. Gurrrola, H. & Minster, J. B. Thickness estimates of the upper-mantle transition zone from bootstrapped velocity spectrum stacks of receiver functions. *Geophys. J. Int.* **133**, 31–43 (1998).
21. Niu, F. & Kawakatsu, H. Complex structure of the mantle discontinuities at the tip of the subducting slab beneath the Northeast China: a preliminary investigation of broadband receiver functions. *J. Phys. Earth* **44**, 701–711 (1996).
22. Revenaugh, J. & Jordan, T. H. Mantle layering from ScS reverberations: 2. The transition zone. *J. Geophys. Res.* **96**, 19763–19780 (1991).
23. Shearer, P. M. & Flanagan, M. P. Seismic velocity and density jumps across the 410- and 660-kilometer discontinuities. *Science* **285**, 1545–1548 (1999).
24. Anderson, D. L. *Theory of the Earth* (Blackwell Science, Oxford, 1989).
25. Bina, C. R. & Helffrich, G. Phase transition Clapeyron slopes and transition zone seismic discontinuities. *J. Geophys. Res.* **99**, 15853–15860 (1994).

## Acknowledgements

We thank the IRIS Data Management Center for data availability and S. van der Lee for expedient delivery and usage of the NA95 velocity model, and K. Dueker for allowing us to use his western USA tomography model before publication. This work was partially supported by the NSF.

Correspondence and requests for materials should be addressed to H.G.

## Are lemmings prey or predators?

P. Turchin\*, L. Oksanen†, P. Ekerholm‡, T. Oksanen‡ & H. Henttonen§

\* Department of Ecology and Evolutionary Biology, University of Connecticut, Storrs, Connecticut 06269, USA

† Department of Ecological Botany, Umeå University, S-901 87 Umeå, Sweden

‡ Department of Animal Ecology, Umeå University, S-901 87 Umeå, Sweden

§ Finnish Forest Research Institute, Vantaa Research Center, PO Box 18, FIN-01301 Vantaa, Finland

Large oscillations in the populations of Norwegian lemmings have mystified both professional ecologists and lay public<sup>1–3</sup>. Ecologists suspect that these oscillations are driven by a trophic mechanism<sup>4,5</sup>: either an interaction between lemmings and their food supply, or an interaction between lemmings and their predators. If lemming cycles are indeed driven by a trophic interaction, can we tell whether lemmings act as the resource ('prey') or the consumer ('predator')? In trophic interaction models, peaks of resource density generally have a blunt, rounded shape, whereas peaks of consumer density are sharp and angular. Here we have applied several statistical tests to three lemming datasets and contrasted them with comparable data for cyclic voles. We find that vole peaks are blunt, consistent with their cycles being driven by the interaction with predators. In contrast, the shape of lemming peaks is consistent with the hypothesis that lemmings are functional predators, that is, their cycles are driven by their interaction with food plants. Our findings suggest that a single mechanism, such as interaction between rodents and predators, is unlikely to provide the 'universal' explanation of all cyclic rodent dynamics.

Many models of resource–consumer interactions predict that population cycles of the two species will be characterized by distinct shapes: blunt rounded peaks for resources, and sharp angular peaks in the consumer density (Fig. 1). This general pattern arises in

predator–prey<sup>6–8</sup> and host–parasitoid<sup>9</sup> models, but is particularly prominent in models developed specifically for small rodents<sup>10–13</sup> for the following reason. Models of interaction between rodents and their specialized predators, weasels<sup>10–12</sup>, must include a self-limitation term in the prey equation (without rodent self-limitation no cycle can occur because the rodent population will escape predator control by virtue of their much higher rate of population growth). A typical rodent–predator cycle occurs as follows. Starting from low prey and predator numbers, prey density rapidly builds up to the point where its further growth is prevented by self-limitation mechanisms, such as social interactions. Predators, on the other hand, can start increasing only after prey density grows beyond the threshold where predators can maintain positive energy balance (this threshold is related to the half-saturation constant in the predator functional response). By the time predators have increased to the point where they cause prey to decline, prey population has spent a prolonged period of time at peak densities. As a result, the shape of prey peaks will be blunt. By contrast, predator population grows exponentially while prey density is above the threshold, followed by rapid declines caused by starvation (or emigration). As a result, predator trajectories are characterized by ‘saw-shaped’ dynamics with sharp peaks. Models in which rodents are consumers<sup>10,13</sup> behave in essentially the same manner, except that it is now rodent trajectories that are characterized by sharp peaks.

We emphasize that distinctive topological features of prey versus predator cycles are a generic feature of two-species trophic models (and are robust with respect to adding stochasticity). Predator peaks must be sharp: we cannot ‘flatten’ them by adding predator self-limitation, because this leads to a loss of cycles (stabilization of the

system). The bluntness of prey peaks is more variable, as the length that prey spent at the upper density threshold will depend on the relative growth rates of prey and predators. If prey growth rate is similar to (or slower than) that of predators, it may be difficult in practice to detect the plateau phase in prey dynamics. Because rodents are characterized by much faster reproductive rates than their predators, however, peak topology should be a particularly useful diagnostic for their dynamics.

Rodent–vegetation models have been applied to lemmings<sup>13</sup>, but unlike the vole case, we still lack good parameter estimates for these models, or manipulative experiments to test rival hypotheses. The theoretical observations discussed above, however, allow us to design an empirical test to distinguish between the two rival hypotheses for lemming cycles: one invoking the interaction with the food supply, and the other with predators. To pursue this idea, we located all time series data on the population dynamics of Norwegian lemmings (*Lemmus lemmus*) that were at least 20 years in length and had at least 2 observations per year (see Methods). We also analysed a comparable set of three vole series from the northern-most part of Fennoscandia (latitude  $\geq 68^\circ\text{N}$ ), where vole populations exhibit high-amplitude oscillations.

Visual examination of the data plotted on logarithmic scale suggests a striking difference between the lemming and vole time series (Fig. 2). Lemmings have very sharp peaks, with rarely more than one observation period at the peak, whereas vole populations spend  $\sim 2$  years in the vicinity of maximum densities before their populations collapse. One way to test statistically whether this difference is real is to examine the frequency distribution of log-transformed densities. The distribution of prey densities should be characterized by a negative skewness (a few observations at very low density, but most near the maximum density). Predator distribution, on the other hand, should be symmetric (no skewness). Indeed, there is a statistically significant difference between skewness of lemming and vole data (Table 1). Another way to look at the same issue is to compute the annual rate of population increase preceding peak density,  $r_{\text{pre-peak}}$ , which should be near zero for the resource, but much greater than zero for the consumer population. This is precisely the pattern that we see (Table 1). These results are therefore consistent with the hypothesis that lemmings are functional predators, whereas voles are functional prey.

An additional feature of numerical dynamics, the variability of peak densities, provides a further clue about dynamical mechanisms that may be responsible for lemming and vole cycles. Prey should have rather stereotypical dynamics at the population peak because they hit the population ceiling imposed by density-dependent regulation. In contrast, predator dynamics do not have a comparable ‘hard ceiling’ because predator density will start to decline when predators run out of food, and when this occurs depends very much on the timing of predator increase with respect to seasonality. Consider a threshold predator density,  $N_{\text{threshold}}$ , above which predators are expected to run out of winter food supply and

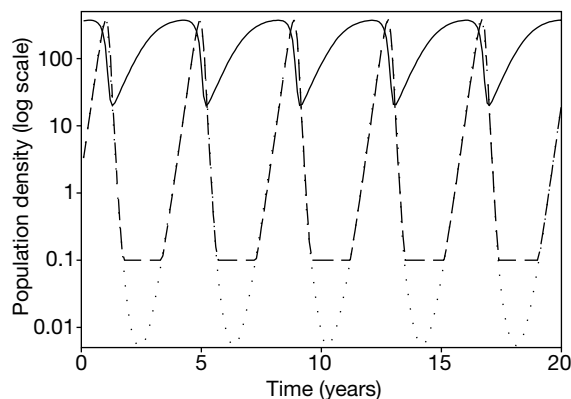


**Figure 1** Shape of predator and prey peaks in a theoretical model<sup>6</sup>. Solid curve shows prey density. Dotted curve shows predator density. Broken line is the predator trajectory that would be observed when there is a threshold below which predator density is undetectable. Note the log scale of the y axis (thus, exponential growth/decline periods are represented by linear segments in the curves).

**Table 1 Results of statistical analyses**

	Skewness			Peak characteristics		
	Log-transformed	Log-transformed, zeroes omitted	Not log-transformed	Mean $r_{\text{pre-peak}}$	$n$	CV of peak density
Lemmings						
Finse	0.33	0.40	3.80	3.420	6	1.360
Kilpisjärvi	1.44	-0.15	4.15	2.966	4	0.805
Finnmark	0.76	0.96	4.32	3.030	2	0.845
Voles						
Kilpisjärvi	-0.80	-0.50	1.21	0.593	9	0.311
Pallasjärvi	-1.18	-0.56	1.56	0.361	4	0.430
Finnmark	-0.57	-0.57	1.38	0.692	4	0.339
$t$ -test statistic	3.412	2.948	14.701	15.016		3.529
$P$	0.027	0.042	0.0001	0.0001		0.024

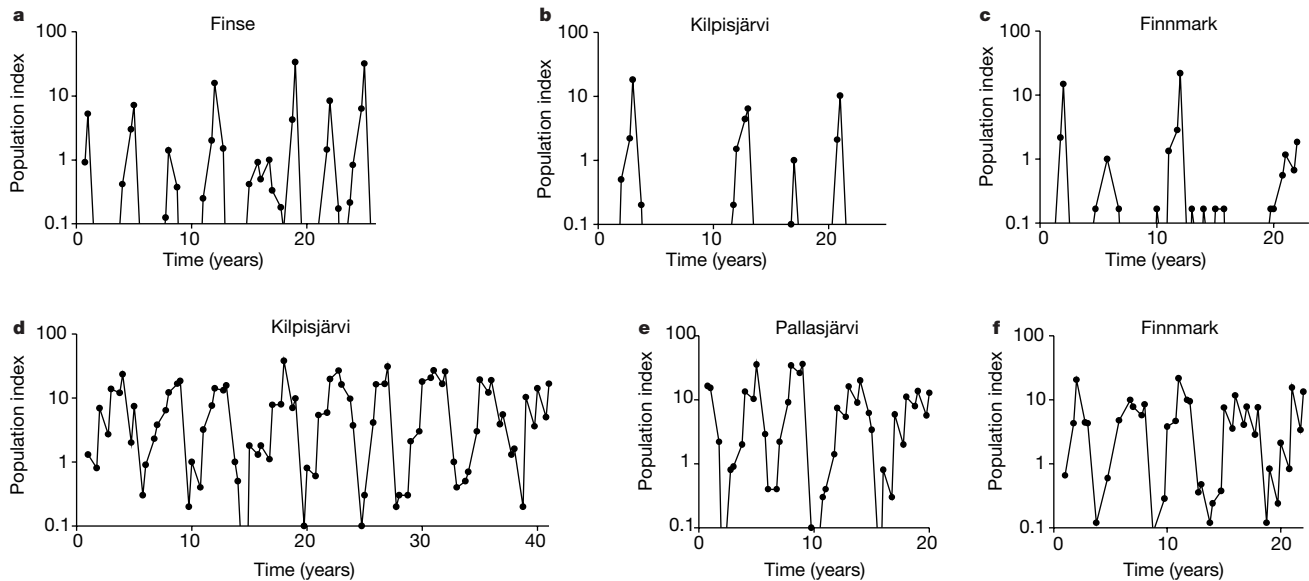


**Figure 2** Population dynamics of lemmings at Finse (a), Kilpisjärvi (b) and Finnmark (c), and of voles at Kilpisjärvi (d), Pallasjärvi (e) and Finnmark (f).

therefore experience a winter crash. If this threshold is reached in the fall, then peak density would be equal to  $N_{\text{threshold}}$ . However, if  $N_{\text{threshold}}$  is achieved in the spring, then predator density will increase much beyond it before the winter crash. As a result, peak density of predators should be highly variable (in fact, this mechanism, the interaction between seasonality and predator–prey dynamics, is at the root of mathematical chaos that may arise in rodent population models<sup>11,14,15</sup>). Again, numerical results are consistent with our main hypothesis (Table 1).

Our findings, which suggest different causal mechanisms for lemming versus vole cycles, concur with what we know about the biology of these rodents. Voles are folivores. Their food plants regrow rapidly after defoliation<sup>16</sup> by mobilizing energy stored underground, and this feature of the vole–vegetation interaction is strongly stabilizing<sup>13</sup>. Lemmings, in contrast, are moss-eaters (particularly so during the critical winter period). Mosses regrow slowly after being depleted by herbivores, and the inherent time lag in this process is highly destabilizing<sup>13</sup>. Furthermore, unlike in more productive vole habitats, lemmings tend to deplete their forage in high arctic and alpine habitats before their predators can reach densities high enough to affect their dynamics. It has been proposed<sup>17</sup> that the dominant consumer–resource interaction in terrestrial grazing webs shifts from the herbivore–plant interface in low productivity systems (lemmings) to the predator–prey interface in higher productivity locations (voles). This view is strongly supported by observations of the strong impact of lemmings on their food supply during peak years<sup>18–20</sup>. Furthermore, lemmings are much more mobile during population peaks and collapses than voles<sup>21</sup>. This observation makes sense within the framework of the hypothesis that we advocate here. Because vole crashes are caused by predators, moving is futile, and can only increase the risk of being eaten. Lemmings, in contrast, have to move during peak density because they face a desperate shortage of food resources.

Historically, population ecologists tended to look for ‘universal’ explanations of the population dynamics of small rodents<sup>3</sup>. As a result, when the view gained ground that dynamics of voles *Microtus agrestis* in Fennoscandia are explained by their interactions with specialist and generalist predators<sup>11,22–25</sup>, it could be argued that lemming cycles are also driven by their predators. Predation hypothesis, however, makes a specific prediction about the topology of lemming cycles, which is at variance with the empirically observed patterns. Thus, our analytical results indicate that popula-

tion oscillations in lemmings and voles may be driven by very different ecological mechanisms. □

**Methods**

**Sources of data**

Voles: Kilpisjärvi and Pallasjärvi<sup>26</sup>, Finnmark<sup>27</sup>. Lemmings: Finse<sup>5,28</sup>, Kilpisjärvi (H.H., unpublished data), Finnmark<sup>27</sup>. Finse and Finnmark lemming data were collected in alpine highlands (the optimal lemming habitat), but Kiplisjärvi data were collected in a birch forest (surrounded by large alpine areas). Birch forest probably constitutes a sink habitat for lemmings, and therefore primarily reflects the lemming dynamics in the surrounding alpine habitat, as indicated by comparing this dataset to once-a-year trapping results from the alpine zone<sup>29,30</sup>.

**Statistical analyses**

**Skewness.** Our theoretical prediction is that log-transformed prey numbers should be negatively skewed, whereas consumers should not be skewed. However, if there are many zero-density observations, and these are assigned to some arbitrary low positive number (which is the standard practice in the analysis of population time-series data; see broken line in Fig. 1), then we should observe an (artificial) positive skewness. The first column in Table 1 (‘log-transformed’) reports the skewness of log-transformed data where zeros are replaced with 0.01; the second column reports the skewness of the frequency distribution of data with zeros omitted; the third column reports the skewness of non-transformed data (where no special handling of zeros is needed). In all cases, vole skewness is significantly less than that for lemmings, as judged by a *t*-test with 4 degrees of freedom. **Pre-peak rate of increase.** This was calculated according to  $r_{\text{pre-peak}} = \ln N_1 - \ln N_2$ , where  $N_1$  is the density during the peak year, and  $N_2$  is the density of the year before. We defined peak as the year with highest geometric mean of spring and fall density (but other reasonable definitions of peak did not affect the main result). The column ‘*n*’ reports the number of peaks on which  $r_{\text{pre-peak}}$  means are based.

**Variability in peak density.** Using the same definition of peaks as above, we calculated the coefficient of variation (standard deviation divided by the mean) of peak densities for each data series.

Received 15 November 1999; 7 April 2000.

1. Elton, C. S. Periodic fluctuations in the number of animals: their causes and effects. *Br. J. Exp. Biol.* **2**, 119–163 (1924).
2. Stenseth, N. C. & Ims, R. A. in *The Biology of Lemmings* (eds Stenseth, N. C. & Ims, R. A.) 3–34 (Linnean Society, London, 1993).
3. Chitty, D. *Do Lemmings Commit Suicide? Beautiful Hypothesis and Ugly Facts* (Oxford Univ. Press, New York, 1996).
4. Stenseth, N. C. & Ims, R. A. in *The Biology of Lemmings* (eds Stenseth, N. C. & Ims, R. A.) 61–96 (Linnean Society, London, 1993).
5. Stenseth, N. C., Chan, K. S., Framstad, E. & Tong, H. Phase- and density-dependent population dynamics in Norwegian lemmings: interaction between deterministic and stochastic processes. *Proc. R. Soc. Lond. B* **265**, 1957–1968 (1998).
6. Rosenzweig, M. L. & MacArthur, R. H. Graphical representation and stability conditions of predator–prey interaction. *Am. Nat.* **97**, 209–223 (1963).
7. May, R. M. in *Theoretical Ecology: Principles and Applications* (ed. May, R. M.) 78–104 (Sinauer Associates, Sunderland, Massachusetts, 1981).

8. Bazykin, A. D., Berezhovskaya, F. S., Denisov, G. A. & Kuznetsov, Y. A. The influence of predator saturation effect and competition among predators on predator-prey system dynamics. *Ecol. Mod.* **14**, 39–57 (1981).
9. Beddington, J. R., Free, C. A. & Lawton, J. H. Dynamic complexity in predator-prey model framed in simple difference equations. *Nature* **225**, 58–60 (1976).
10. Oksanen, L. Exploitation ecosystems in seasonal environments. *Oikos* **57**, 14–24 (1990).
11. Hanski, I., Turchin, P., Korpimäki, E. & Henttonen, H. Population oscillations of boreal rodents: regulation by mustelid predators leads to chaos. *Nature* **364**, 232–235 (1993).
12. Turchin, P. & Hanski, I. An empirically-based model for the latitudinal gradient in vole population dynamics. *Am. Nat.* **149**, 842–874 (1997).
13. Turchin, P. & Batzli, G. Availability of food and the population dynamics of arvicoline rodents. *Ecology* (in the press).
14. Oksanen, L. & Oksanen, T. Long-term microtine dynamics in north fennoscandian tundra—the vole cycle and the lemming chaos. *Ecography* **15**, 226–236 (1992).
15. Turchin, P. Chaos and stability in rodent population dynamics: evidence from nonlinear time-series analysis. *Oikos* **68**, 167–172 (1993).
16. Ostfeld, R. S., Canham, C. D. & Pugh, S. R. Intrinsic density-dependent regulation of vole populations. *Nature* **366**, 259–261 (1993).
17. Oksanen, L., Fretwell, S. D., Arruda, J. & Niemela, P. Exploitation ecosystems in gradients of primary productivity. *Am. Nat.* **118**, 240–261 (1981).
18. Batzli, G. O., White, R. G., MacLean, S. F., Pitelka, F. A. & Collier, B. D. in *An arctic ecosystem: the coastal tundra at Barrow, Alaska*. (eds Brown, J., Miller, P. C., Tieszen, L. L. & Bunnell, F. L.) 335–410 (Hutchinson and Ross, Stroudsburg, PA, 1980).
19. Chernyavsky, F. B. & Tkachev, A. V. *Population Cycles of Lemmings in the Arctic: Ecological and Endocrine Aspects* (in Russian) (Nauka, Moscow, Russia, 1982).
20. Moen, J., Lundberg, P. A. & Oksanen, L. Lemming grazing on snowbed vegetation during a population peak. *Arctic Alpine Res.* **25**, 130–135 (1993).
21. Henttonen, H. & Kaikusalo, A. in *The Biology of Lemmings* (eds Stenseth, N. C. & Ims, R. A.) 157–186 (Academic, London, 1993).
22. Hansson, L. & Henttonen, H. Gradients in density variations of small rodents: the importance of latitude and snow cover. *Oecologia* **67**, 394–402 (1985).
23. Hanski, I., Hansson, L. & Henttonen, H. Specialist predators, generalist predators, and the microtine rodent cycle. *J. Anim. Ecol.* **60**, 353–367 (1991).
24. Hanski, I., Henttonen, H., Korpimäki, E., Oksanen, L. & Turchin, P. Small rodent dynamics and predation. *Ecology* (in the press).
25. Korpimäki, E. & Norrdahl, K. Experimental reduction of predators reverses the crash phase of small-rodent cycles. *Ecology* **79**, 2448–2455 (1998).
26. Henttonen, H. & Hanski, I. in *Chaos in Real Data* (eds Perry, J. N., Smith, R. H., Woivod, I. P. & Morse, D.) 73–96 (Kluwer Academic, Dordrecht, Netherlands, 2000).
27. Ekerholm, P., Oksanen, L. & Oksanen, T. Long-term dynamics of voles and lemmings in low arctic tundra and above the willow limit as a test of theories on trophic interactions. *Ecography* (in the press).
28. Framstad, E., Stenseth, N. C., Bjørnstad, O. N. & Falck, W. Limit cycles in Norwegian lemmings: tensions between phase-dependence and density dependence. *Proc. R. Soc. Lond. B* **264**, 31–38 (1997).
29. Henttonen, H., Kaikusalo, A., Tast, J. & Viitala, J. Interspecific competition between small rodents in subarctic and boreal ecosystems. *Oikos* **29**, 581–590 (1977).
30. Virtanen, R., Henttonen, H. & Laine, K. M. Lemming grazing and the structure of snowbed plant community—a long-term experiment at Kilpisjärvi, in Finnish Lapland. *Oikos* **79**, 155–166 (1997).

**Acknowledgements**

We thank I. Hanski and N. C. Stenseth for valuable discussion and comments on the manuscript.

Correspondence and requests for materials should be addressed to P.T. (e-mail: Peter.Turchin@UConn.edu).

**Highly fecund mothers sacrifice offspring survival to maximize fitness**

**Sigurd Einum\*† & Ian A. Fleming\***

\* Norwegian Institute for Nature Research, Tungasletta 2, N-7485 Trondheim, Norway

† Department of Zoology, Norwegian University of Science and Technology, N-7034 Trondheim, Norway

Why do highly fecund organisms apparently sacrifice offspring size for increased numbers when offspring survival generally increases with size<sup>1–3</sup>? The theoretical tools for understanding this evolutionary trade-off between number and size of offspring have developed over the past 25 years<sup>1,4–10</sup>; however, the absence of data on the relation between offspring size and fitness in highly fecund species, which would control for potentially confounding variables, has caused such models to remain largely

hypothetical<sup>11,12</sup>. Here we manipulate egg size, controlling for maternal trait interactions, and determine the causal consequences of offspring size in a wild population of Atlantic salmon. The joint effect of egg size on egg number and offspring survival resulted in stabilizing phenotypic selection for an optimal size. The optimal egg size differed only marginally from the mean value observed in the population, suggesting that it had evolved mainly in response to selection on maternal rather than offspring fitness. We conclude that maximization of maternal fitness by sacrificing offspring survival may well be a general phenomenon among highly fecund organisms.

One of the most intensely studied maternal traits is egg size, owing to its direct consequences for offspring fitness<sup>1,3</sup>. Individual mothers are forced to trade off offspring quantity against quality during reproduction<sup>13,14</sup>. Much of the theoretical work on this question of reproductive allocation has focused around the seminal paper of Smith and Fretwell<sup>4</sup>. Because of the trade-off between egg size and number, their model predicts the evolution of an optimal egg size that maximizes maternal fitness (product of number of offspring and their fitness), with mothers having the upper hand in this parent-offspring conflict. This potentially explains the existence of species experiencing massive mortality during juvenile stages, because offspring survival rates that maximize maternal fitness may be low compared with those maximizing offspring fitness. When considering the impact that the Smith-Fretwell model has had on aspects of life-history theory<sup>1,5–10</sup>, it is worrying that empirical support from highly fecund species is lacking. The general validity of the Smith-Fretwell model has previously been questioned on the basis of data from organisms producing few offspring<sup>12</sup>, and it has been criticized for being too simplistic<sup>11</sup>.

We therefore undertook an experimental field study using Atlantic salmon to test empirically whether maternal or offspring fitness is maximized in highly fecund species (egg numbers range from 1,791 to 18,847)<sup>15</sup>. Egg size was manipulated by rearing females to adulthood in captivity. This procedure resulted in some females producing highly variable egg sizes (mean coefficient of variation = 18.5%) relative to that found in the wild (4.0%; S.E. and I.A.F., unpublished data). A sample of small and large eggs from each of eight females was fertilized by one male, producing a total of eight pairs of full-sib groups. At the eyed stage, equal numbers of small and large eggs within a pair were buried in separate artificial gravel nests<sup>3</sup>, producing a total of 16 such nests. Small eggs were on average 31.4% lighter than their large siblings ((mean ± s.d.) small: 85.4 ± 15.1 mg; large: 125.4 ± 13.4 mg;  $t_7 = 6.06$ ,  $P = 0.001$ , paired samples  $t$ -test). The size separation within family groups was responsible for 69.2% of the total variation in egg size within the population, randomizing the effects of other maternal or genetic traits potentially correlated with egg size. Thus, this design allowed us to test for a causal relationship between egg size and offspring fitness<sup>16,17</sup>. It excluded the possible effects of interactions with other maternal traits that may cause the optimum egg size to vary among females within natural populations<sup>1,6,18</sup>. Juveniles emerging from the nests were released in a natural stream, and were sampled 28 and 107 d after median emergence to assess their success.

**Table 1 Selection on egg size for Atlantic salmon**

	$\beta$	$\beta'$	$P$	$\gamma$	$\gamma'$	$P$
Offspring survival	19.65 (5.05)	0.488 (0.126)	0.001	-573.8 (343.5)	-14.30 (8.54)	0.069
Maternal RS	14.43 (5.85)	0.358 (0.145)	0.009	-723.7 (305.5)	-18.02 (7.59)	0.023

Selection gradients relate relative offspring survival and maternal reproductive success (RS, proportion offspring survival × potential maternal fecundity) to egg size. Directional selection gradients (unstandardized,  $\beta$ ; standardized,  $\beta'$ ) are estimated from linear regression coefficients, and nonlinear (stabilizing) selection gradients (unstandardized,  $\gamma$ ; standardized,  $\gamma'$ ) are estimated from regression coefficients of squared deviations from the mean<sup>21</sup>. Standard errors are indicated in parentheses. Residuals from regressions between the traits and log-transformed fitness measures proved to be normally distributed, allowing parametric tests of significance<sup>21</sup>.